



Patient-Specific Radiation Dosimetry for Radionuclide Therapy of Liver Tumors With Intrahepatic Artery Rhenium-188 Lipiodol

Pat B. Zanzonico, PhD,* and Chaitanya Divgi, MD^{†,1}

A clinically practical algorithm has been developed for the treatment of liver cancer by the administration of rhenium-188 (¹⁸⁸Re)-labeled lipiodol via the hepatic artery. This algorithm is based on the “maximum tolerated-activity” paradigm for radionuclide therapy. A small “scout” activity of ¹⁸⁸Re-labeled lipiodol is administered to the patient before the actual therapeutic administration. At approximately 3 hours after administration, the activities in the normal liver, liver tumors, lungs, and total body are measured by gamma camera imaging using the conjugate-view method, with first-order corrections for attenuation (using a ¹⁸⁸Re transmission scan) and scatter (using the “dual-window” method). At the same time, peripheral blood samples are counted, and the activity concentrations in whole blood are calculated. The blood activity concentrations are then converted to red marrow activity concentrations and then total red marrow activity using anatomic data from Standard Man anthropomorphic models. Next, the cumulated activities in the normal liver, liver tumors, lungs, red marrow, and total body are calculated using the measured activities in the respective source regions and conservatively assuming elimination of activity only by physical decay in situ. The absorbed doses to the therapy-limiting normal tissues, liver, lung, and red marrow, are then calculated using the Medical Internal Radiation Dose Committee schema, adjusting the pertinent S factors for differences in total body and organ masses between the patient and the anthropomorphic model and including the dose contribution from the liver tumors. Finally, based on maximum tolerated absorbed doses of 3,000, 1,200, and 150 rad (cGy) to liver, lung, and red marrow, the respective absorbed doses per unit administered activity are used to calculate the therapy activity. Although not required for treatment planning, tumor absorbed dose may also be estimated. This algorithm has been automated using an Excel (Microsoft, Redmond, WA) spreadsheet. *Semin Nucl Med* 38:S30-S39 © 2008 Elsevier Inc. All rights reserved.

Historically, nuclear medicine has been largely a diagnostic specialty, and relatively low administered activities that are used diagnostically yield important clinical information whose benefit far outweighs the small potential risk associated with the attendant low normal-tissue absorbed doses. Average normal tissue doses for the “standard” patient, as found in package inserts for approved radiopharmaceuti-

cals and in “reports” issued, for example, by the International Commission on Radiological Units, are therefore entirely adequate, although the tissue doses received by particular patients may deviate rather widely from such averages.

By incorporating appropriate radionuclides in appropriately large amounts into target tissue-avid radiopharmaceuticals, a sufficiently high radiation dose may be delivered to produce a therapeutic response in tumor or other target tissue, as in rhenium-188 (¹⁸⁸Re)-labeled lipiodol therapy for the treatment of liver cancer. With such greater administered activities and resulting greater normal-tissue doses, serious radiation injury may ensue. It becomes critical, then, to determine at-risk normal tissue radiation doses with reasonable accuracy and precision. In conjunction with reliable dose-toxicity relationships for normal tissues, these dose estimates can be used to plan safe and effective radionuclide treatment for individual patients. Perhaps because of the greater accu-

*Department of Medical Physics, Memorial Sloan-Kettering Cancer Center, New York, NY.

†Department of Radiology, Memorial Sloan-Kettering Cancer Center, New York, NY.

¹Present address: Division of Nuclear Medicine, University of Pennsylvania, Philadelphia, PA.

Conflict of Interest: None.

Address reprint requests to Pat B. Zanzonico, PhD, Department of Medical Physics, Memorial Sloan-Kettering Cancer Center, 1275 York Avenue, New York, NY 10021. E-mail: ZanzoniP@mskcc.org

racy and precision required, dosimetry methods for radionuclide therapy have not yet been standardized. This report describes a clinically practical algorithm for the treatment of liver cancer by hepatic artery administration of ^{188}Re -labeled lipiodol based on the maximum tolerated activity. This algorithm has been automated using an Excel (Microsoft, Redmond, WA) spreadsheet, which performs the necessary calculations and incorporates the pertinent reference data.

Increasingly, to maximize the efficacy and minimize the toxicity of radionuclide therapy and in place of fixed-activity protocols, administered activities are customized to the individual patient. On the basis of kinetic measurements of "scout" activities and absorbed-dose calculations, individual patients will receive the maximum activity that will not exceed the radiation tolerance (ie, the tolerance absorbed dose) of normal tissue. Typically, perhaps only several normal tissues will be at significant risk, that is, likely to receive absorbed doses approaching their respective tolerance dose. For the treatment of metastatic thyroid cancer with iodide-131 (^{131}I), for example, the therapeutic administered activity is that calculated to deliver no more than 200 rad to blood (as a surrogate for bone marrow).¹⁻⁵ In radioimmunotherapy of non-Hodgkin's B-cell lymphoma with ^{131}I -labeled B1 anti-CD20 monoclonal antibody, on the other hand, the therapeutic administered activity is that delivering a dose of 75 rad to the total body (again as a surrogate for bone marrow).⁶⁻⁹ For ^{188}Re -labeled lipiodol administered via the hepatic artery, the at-risk normal tissues are liver, lung, and red marrow and their respective tolerance absorbed doses are 3,000, 1,200, and 150 rad. Thus, for a particular patient, based on the empirically determined absorbed dose per unit administered activity (rad/mCi or cGy/MBq) to the liver, lung, and red marrow, the therapeutic administered activity will be the lowest value among those activities projected to deliver 3,000 rad to the liver, 1,200 rad to the lung, and 150 rad to the red marrow.

The dosimetry methodology described was used in a therapy trial conducted under the auspices of the International Atomic Energy Agency's Thematic/Doctoral Coordinated Research Project, entitled "Management of Liver Cancer Using Radionuclide Methods With Special Emphasis on Trans-Arterial Radioconjugate Therapy and Internal Dosimetry." The trial was unique in that a single protocol using a common labeling procedure for ^{188}Re lipiodol and dosimetric methodology was conducted in 8 countries across 2 continents.

Physical Properties of ^{188}Re

^{188}Re , with a physical half-life ($(T_{1/2})_p$) of 17 hours and physical decay constant (λ_p) of 0.041 hours, decays by negatron (β -ray) emission.¹⁰ The most abundant β -rays have maximum energies of 0.53 to 0.709 MeV and therefore ranges in water and soft tissue of ~ 4 mm. Such relatively energetic β -rays are dosimetrically well-suited to treat primary liver tumors. Their relatively long range, ~ 4 mm, means that tumors will be rather uniformly irradiated. At the same time, because such tumors typically have dimensions of at least several centimeters at the time of treatment, these β -rays will

be completely absorbed within the tumors. As usual, therefore, the tumor-to-tumor, or "self-irradiation," β -ray absorbed fraction will be one, $\phi_{np}(\text{tumor} \leftarrow \text{tumor}) = 1$, where "np" indicates "nonpenetrating" radiation (ie, particulate radiations such as β -rays).

In addition, ^{188}Re emits a 155-keV γ -ray in 15% of its decays as well as 478- and 633-keV γ -rays (2.3%). For dosimetry measurements, the 155-keV γ -ray, comparable in energy with the 140-keV γ -ray of technetium-99m (^{99m}Tc), can be imaged with a conventional gamma camera using a standard 20% photopeak energy window, $155 \text{ keV} \pm 10\% = 150$ to 171 keV. A low-energy collimator, however, would not be suitable for imaging ^{188}Re . Although low in abundance, the scattered 478- and 633-keV γ -rays would penetrate such a collimator and thus degrade the image by contributing a relatively large number of "uncollimated," mispositioned counts to the ^{188}Re image. Although high-energy collimation would minimize this effect, the associated reduction in sensitivity might be prohibitive since the 155-keV γ -rays are emitted in only 15% of ^{188}Re decays. Thus, medium-energy collimation is probably the optimum choice for imaging ^{188}Re . Depending on the make and model of the gamma camera, the so-called "front-end" (ie, preamplifier, amplifier, and/or high-voltage) settings used for ^{99m}Tc can probably be used for ^{188}Re . On the other hand, a separate sensitivity or uniformity (flood) correction map (table) probably should be acquired and used for ^{188}Re . Further, in contrast to conventional practice, a system ^{188}Re correction map, that is, a correction map using a flood, rather than a point, source of ^{188}Re and with collimation in place, should be acquired. In this way, the confounding effects of the 478- and 633-keV γ -rays can be accounted for.

Pharmacokinetics and Cumulated Activities of ^{188}Re -Labeled Lipiodol

After the administration of ^{188}Re -labeled lipiodol into the hepatic artery, uptake in liver tumors and in at-risk normal tissues, such as liver and lung, is rapid. The subsequent clearance of lipiodol is remarkably slow (biological clearance half-times range from ~ 8 days in tumor to ~ 13 days in lung and liver)¹¹ and, other than liver, tumor, and lung, there are no notable sites of lipiodol accumulation.¹² The appearance of activity in blood and therefore presumably in red marrow is somewhat slower but still rapid, generally reaching maximal or near-maximal levels by 3 to 4 hours after administration. Therefore, relative to the 17-hour physical half-life of ^{188}Re , uptake may be considered instantaneous followed by elimination only by physical decay in situ (ie, there is negligibly slow biological elimination) in blood (red marrow) as well as in liver and lung. This means that ^{188}Re activity in the respective tissues (source regions) follows monoexponential kinetics in which (1) the zero-time-activity can be reliably estimated for liver and lung from scintigraphic images acquired anytime up to ~ 3 hours after administration and for red marrow obtained at ~ 3 hours and (2) the effective clearance

constant (or half-times) equals the physical decay constant (or half-time):

$$A_h(t) = (A_o)_h e^{-(\lambda_e)_h t} \quad (1)$$

where $A_h(t)$ = the activity in source region r_h at time t after administration;

$$(A_o)_h = \text{the zero-time activity (uptake) in source region } r_h \\ \approx A_h(3 \text{ hours});$$

$(\lambda_e)_h$ = the effective clearance constant of activity in source region r_h

$$= \lambda_p + (\lambda_b)_h \quad (2a)$$

$$\approx \lambda_p \quad (2b)$$

$$= 0.041/\text{hr for } ^{188}\text{Re} \quad (2c)$$

where λ_p = the physical decay constant of the radionuclide

$$= 0.041/\text{hr for } ^{188}\text{Re} \quad (3)$$

and $(\lambda_b)_h$ = the biological clearance constant from source region r_h .

The resulting monoexponential kinetics, in turn, greatly simplify the estimation of cumulated activities. (The subscript, "1/2," has been eliminated to make the equations less unwieldy.)

$$\bar{A}_h = \frac{(A_o)_h}{(\lambda_e)_h} \quad (4a)$$

$$\approx \frac{(A_o)_h}{\lambda_p} \quad (4b)$$

$$= 1.44 (A_o)_h (T_e)_h \quad (4c)$$

$$\approx 1.44 (A_o)_h T_p \quad (4d)$$

where T_e = the effective half-life

T_p = the physical half-life

$$= 17 \text{ hours for } ^{188}\text{Re} \quad (5)$$

Although consistent with the measured kinetics of ^{188}Re -labeled lipiodol, the assumptions of instantaneous uptake and elimination only by physical decay in situ are nonetheless conservative. That is, these assumptions tend to yield estimates of cumulated activities and therefore absorbed doses per unit administered activity that are likely somewhat greater than the actual values. In turn, the calculated therapeutic administered activity will be slightly lower than the actual maximum-tolerated activity. However, given the large uncertainties in estimating absorbed doses from internal radionuclides, it is probably desirable to err on the side of safety.

Source- and Target-Region Masses

For ^{188}Re -lipiodol, the source regions are liver, lung, red marrow, and the rest of the body, and the pertinent target regions

are liver, lung, and red marrow. In addition to total body mass, liver and tumor masses (in g) are required for each patient before treatment. The most expeditious and accurate approach to liver and volumetrics is either the use of computed tomography (CT) or magnetic resonance imaging (MRI). The CT or MRI images themselves are not required for dosimetry—only the estimates of the liver and masses. For purposes of treatment planning, gamma camera imaging in general and planar gamma camera imaging in particular are not really adequate for such volumetric measurements. Measurement of patient-specific lung and red marrow masses are not required because the effect of mass on the respective S factors can be reasonably approximated using the patient's total-body mass (see below "Calculation of Absorbed Doses: The Medical Internal Radiation Dose Committee (MIRD) Schema"). On the other hand, measurement of the liver and the intrahepatic lesions is required not only because these lesions are critical source and target regions but also because they may significantly distort the overall size and shape of the liver. On each transverse CT or MR image j on which the liver and/or the liver tumors appear, regions of interest (ROIs) may be manually drawn around the entire liver (including the tumors) and around each individual lesion. The masses of the entire liver (including the tumors) and each tumor are then calculated:

Mass of region i (g)

$$= \sum_{\text{Image } j} \text{Area of region } i \text{ in image } j \text{ (pixels)} \\ \times \text{Pixel area (mm}^2) \times \text{Image thickness (mm)} \\ \times \rho(\text{g/cm}^3) \times 0.001 \text{ cm}^3/\text{mm}^3 \quad (6)$$

The mass of the normal liver (ie, the entire liver excluding the liver tumors) can then be calculated:

Mass of normal liver (g)

$$= \text{Mass of entire liver (g)} \\ - \sum_{\text{Liver tumors } k} \text{Mass of liver tumor } k \text{ (g)} \quad (7)$$

An analogous ROI analysis can be applied to the gamma camera images to determine the activities and cumulated activities specifically in the normal liver and the tumor(s).

Source-Region Time-Activity Data

As discussed previously, because of the rapid uptake and subsequent slow clearance of lipiodol relative to the 17-hour physical half-life of ^{188}Re , measurement of liver, lung, and total-body activities can be performed anytime from 1 to 3 hours after administration to yield the respective "zero-time" source-region activities. Blood sampling, on the other hand, should not be performed before ~ 3 hours after administration. All activity or activity concentration measurements must be corrected for radioactive

decay from the time of the ¹⁸⁸Re administration to the time of the measurement.

Quantitation of activity in red marrow presents a special problem in radionuclide dosimetry in that it is widely distributed source region that cannot be assayed in its entirety. At that same time, there may be wide variability in activity concentrations in marrow, and biopsy and counting of activity in a marrow sample are therefore prone to sampling error.¹³ A simple practical approach is based on peripheral blood sampling and counting of a weighed blood sample in a scintillation well counter calibrated for ¹⁸⁸Re. The patient's hematocrit must also be measured. Importantly, for radiopharmaceuticals such as ¹⁸⁸Re-labeled lipiodol, which do *not* localize on or in blood or marrow cells, the activity concentration in blood extracellular fluid (ie, plasma) equals the activity concentration in red marrow extracellular fluid at equilibrium.^{14,15} Therefore, the red marrow activity concentration can be calculated as follows.^{14,15}

Activity concentration (μCi/g) in red marrow

$$= \frac{\text{Red marrow extracellular fluid fraction}}{1 - \text{Hematocrit}} \times \text{Activity concentration } (\mu\text{Ci/g}) \text{ in blood} \quad (8)$$

For purposes of radionuclide dosimetry, the American Association of Physicists in Medicine has recommended a value of 0.4 for the red marrow extracellular fluid fraction¹⁴ whereas Sgouros has recommended a value of 0.2.¹⁵ The more conservative value of 0.4, which yields a greater red marrow activity concentration, should be used.

Finally, the total activity in red marrow is calculated using the total mass of red marrow in the 70-kg reference man (1,500 g) or 54-kg reference woman (1,300 g) anthropomorphic models for male or female patients,^{16,17} respectively:

Activity (μCi) in red marrow

$$= \text{Total mass (g) of red marrow} \times \text{Activity concentration } (\mu\text{Ci/g}) \text{ in red marrow} \quad (9)$$

¹⁸⁸Re activities in the liver, lung, and the rest of the body can be measured by planar gamma camera imaging using the conjugate-view method with first-order corrections for scatter and attenuation. Optimally, this is performed using a dual-detector gamma camera with whole-body scanning capability.

Scatter Correction

“Small-angle” Compton scatter, which is abundant in a distributed radioactive source such as a patient, diverts emitted x- and γ-rays from their original direction of travel *without* reducing their energy to the point that it lies below the photopeak energy window. As a result, mispositioned events are included in the gamma camera image. Although important for activity quantitation, rigorous scatter cor-

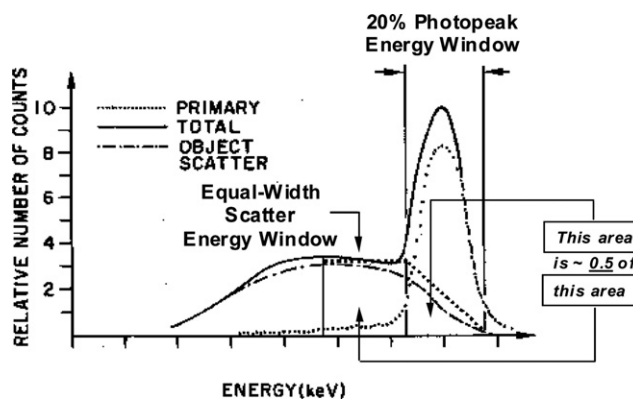


Figure 1 The dual-window scatter correction¹⁹ requires simultaneous acquisition of 2 separate images, 1 corresponding to the conventional photopeak energy window (155 keV ± 10% = 150 – 171 keV in the case of ¹⁸⁸Re) and a second, “scatter” energy window of equal width (in terms of energy (keV)) and immediately below the photopeak energy window (109-139 keV). The multiplicative factor of 0.5 approximates, for the “Object Scatter” spectrum, the triangular area under the curve in the photopeak energy window as a fraction of the rectangular area under the curve in the scatter energy window.

rection is complex.¹⁸ However, Jaszczak and coworkers¹⁹ have developed a straightforward scatter correction method, the so-called “dual-window” method, that can be easily implemented on most modern gamma camera systems. As illustrated in Figure 1, the dual-window scatter correction requires simultaneous acquisition of 2 separate images, corresponding to photopeak (conventional) and scatter energy windows, respectively.

The scatter-corrected image is then derived as follows:

Scatter-corrected image

$$= \text{Photopeak energy window image} - 0.5 \times \text{Scatter energy window image} \quad (10)$$

In all subsequently described image analyses, the scatter corrected images are used.

Attenuation Correction

Attenuation of the 115-keV γ-rays emitted by ¹⁸⁸Re in vivo will be substantial and highly variable, depending on the size (ie, thickness) of the patient and of different internal organs of the patient and the composition (soft tissue, bone, lung [ie, air]) of the overlying tissue. Mean attenuation correction factors should therefore be measured for the pertinent source regions, the liver and liver tumors, lung, and the total body, as illustrated in Figure 2.² A flood source is filled with a uniform ~10-mCi solution of ¹⁸⁸Re and placed on the lower gamma camera detector. With the scanning table in place but *without* the patient, a “whole-body” scan of the flood source is acquired with the same scan speed, scan length, and detector separation as will be used for the transmission scan. Before the administration of radioactivity to the patient, a ¹⁸⁸Re transmission scan

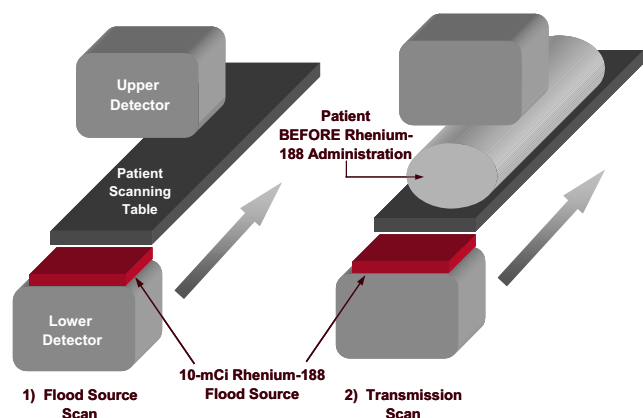


Figure 2 Setup for gamma camera imaging for measurement of mean attenuation correction factors.² As in conventional whole-body scanning, the upper and lower detectors are translated together relative to the patient scanning table. (Color version of figure is available online.)

through the patient is acquired; the administration of the ^{188}Re -labeled lipiodol and subsequent ^{188}Re imaging should be performed without moving the patient. Mean attenuation correction factors for the pertinent source regions, the liver and liver tumors, lung, and total body, are then formed from the 2 upper detector scans by region-of-interest (ROI) analysis:

Mean attenuation correction factor for source region r_h

$$= \sqrt{\frac{\text{Mean counts per pixel in source region } r_h \text{ ROI on the upper detector flood source scan}^*}{\text{Mean counts per pixel in source region } r_h \text{ ROI on the upper detector transmission scan}^*}} \quad (11)$$

*Scatter-corrected image.

The ROI for the liver and liver tumors can be manually drawn on the subsequently acquired ^{188}Re images of the patient and the lung and total body ROIs on the transmission scan.

Conjugate-View Imaging

Once the patient has been injected with the ^{188}Re -labeled lipiodol, a calibrated standard source of ^{188}Re is placed on the patients scanning table adjacent to but not on the patient and a whole-body scan performed (Fig. 3).

Both the upper- and lower-detector images should be corrected for scatter (see Fig. 3 and Eq. 10), the scatter-corrected lower-detector image “mirrored” to align it with the upper detector image, and the geometric mean image formed:

Geometric-mean image

$$= \sqrt{\text{Upper-detector image}^* \times \text{Lower-detector image}^{**}} \quad (12)$$

*Scatter-corrected image.

**Scatter-corrected, mirrored image.

Forming the geometric-mean image largely eliminates the distance dependence of the detected count rate.

Based on the net (ie, background-corrected) counts in the geometric-mean image of the calibrated standard, the ^{188}Re system calibration factor is then calculated:

^{188}Re system calibration factor (counts/ μCi)

$$= \frac{\left(\text{Total pixels in calibrated standard ROI} \times \{ \text{Mean counts per pixels in calibrated standard ROI} - \text{Mean counts per pixel in background ROI} \} \right)}{\text{Activity } (\mu\text{Ci}) \text{ in calibrated standard ROI}} \quad (13)$$

Finally, the activity (μCi) in each of the pertinent source regions r_h , liver, tumor(s), lung, and total body, is calculated using ROI analysis of the geometric-mean image:

Activity (μCi) in source region r_h

Mean attenuation correction factor for source region r_h

$$\times \frac{\left(\text{Total pixels in source region } r_h \text{ ROI} \times \{ \text{Mean counts per pixels in source region } r_h \text{ ROI} - \text{Mean counts per pixel in background ROI} \} \right)}{{}^{188}\text{Re system calibration factor (counts}/\mu\text{Ci)}} \quad (14)$$

Calculation of Absorbed Doses: The Medical Internal Radiation Dose Committee (MIRD) Schema

The basic absorbed dose calculation in the MIRD schema, yielding the *mean* absorbed dose to target region r_k from the

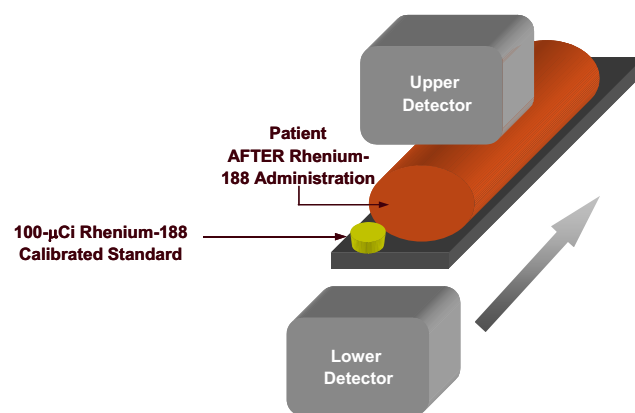


Figure 3 Set-up for conjugate-view whole-body scanning following administration of the ^{188}Re -labeled lipiodol, with a ^{188}Re -calibrated standard ($\sim 100 \mu\text{Ci}$) in the field of view.² (Color version of figure is available online.)

activity (ie, cumulated activity) in source region r_h , is as follows:^{2,16,20–22}

$$\bar{D}(r_k \leftarrow r_h) = \frac{\bar{A}_h \sum_i \Delta_i \phi_i(r_k \leftarrow r_h)}{M_k} \quad (15a)$$

$$= \bar{A}_h \sum_i \Delta_i \Phi_i(r_k \leftarrow r_h) \quad (15b)$$

$$= \bar{A}_h S(r_k \leftarrow r_h) \quad (15c)$$

\bar{A}_h = the cumulated activity in source region r_h , that is, the total number of decays in source region r_h ,

M_k = the mass of target region r_k ,

Δ_i = the equilibrium dose constant for radiation i , that is, the average energy emitted per decay in the form of radiation i (see reference 10 for a comprehensive tabulation),¹⁰

$\phi_i(r_k \leftarrow r_h)$ = the absorbed fraction in target region r_k for radiation i emitted in source region r_h , that is, the fraction of energy of radiation i emitted in source region r_h that is absorbed in target region r_k ,

$\Phi_i(r_k \leftarrow r_h)$ = the *specific* absorbed fraction in target region r_k for radiation i emitted in source region r_h , that is, the fraction of energy of radiation i emitted in source region r_h that is absorbed per unit mass in target region r_k

$$\equiv \frac{\phi_i(r_k \leftarrow r_h)}{M_k}, \quad (16)$$

and $S(r_k \leftarrow r_h)$ = the radionuclide-specific S factor for target region r_k and source region r_h , that is, the absorbed dose to target region r_k per unit cumulated activity in source region r_h

$$\equiv \frac{\sum_i \Delta_i \phi_i(r_k \leftarrow r_h)}{M_k} \quad (17)$$

The *total* mean absorbed dose $\bar{D}(r_k)$ to target region r_k is then calculated by summation of the absorbed dose contributions from all source regions r_h :

$$\bar{D}(r_k) = \sum_h \frac{\bar{A}_h \sum_i \Delta_i \phi_i(r_k \leftarrow r_h)}{M_k} \quad (18a)$$

$$= \sum_h [\bar{A}_h \sum_i \Delta_i \Phi_i(r_k \leftarrow r_h)] \quad (18b)$$

$$= \sum_h [\bar{A}_h S(r_k \leftarrow r_h)] \quad (18c)$$

See Tables 1 and 2 for a tabulation of the standard anthropomorphic models used in the MIRD schema and selected ¹⁸⁸Re S factors for the 70-kg standard man model, respectively.

The cumulated activity, \bar{A}_h , in each pertinent source region r_h , liver, lung, red marrow, and total body, is calculated from Eq. (4b) using the respective zero-time activities, $(A_0)_h$, given by Eq. (9) for red marrow and by Eq. (14) for liver, lung, and total body. Finally, the rest-of-

body cumulated activity can be calculated by subtracting the liver, lung, and red marrow cumulated activities from the total body cumulated activity.

Adaptation of the MIRD Schema to Patient-Specific Dosimetry

Although the standard anthropomorphic models used in the MIRD schema represent normal human anatomy and thus do not include tumors, the schema can be adapted to patient-specific normal-organ dosimetry for planning radionuclide therapy based on the maximum-tolerated activity.² This is the approach adopted for ¹⁸⁸Re-labeled lipiodol treatment of liver cancer. Not surprisingly, the most important quantitative adjustment in this adaptation involves the tumor-bearing organ(s), in this case, the liver.

For organ “non-self” irradiation (source region $r_h \neq$ target region r_k), S factors are relatively insensitive to organ (ie, source- and target-region) size and shape. Therefore, unless the source and/or target regions are grossly abnormal (eg, because of the presence of tumors), the reference man (or reference woman) S factors may be applied to specific patients for calculating the organ non-self absorbed dose contribution:

$$S(r_k \leftarrow r_h) \approx S(r_k \leftarrow r_h) \quad (19)$$

if $r_h \neq r_k$

For organ “self” irradiation (source region $r_h =$ target region r_k), S factors are approximately inversely proportional to organ mass because most of the self-dose to any organ is contributed by nonpenetrating radiations that are completely absorbed locally regardless of the organ mass whereas absorbed dose, by definition, is inversely proportional to the organ mass. Therefore, for normal organ (ie, organs without tumor), S factors adjusted for the difference in mass between the patient and reference-man organ may be applied to specific patients for calculating the self absorbed dose contribution:

$$S(r_k \leftarrow r_h) \approx S(r_k \leftarrow r_h) \times \frac{\text{Reference-man target-region } (r_k) \text{ mass}}{\text{Patient target-region } (r_k) \text{ mass}} \quad (20a)$$

if $r_h = r_k$

In principle, patient organ masses may be estimated with CT or MRI. In practice, however, masses of normal organs may not be available. A more practical, though less accurate, adaptation of Eq. (18a) based on the patient and reference man total-body masses may then be used:

Table 1 The Organs (Source and Target Regions) and Organ Masses of the Age-Dependent Anthropomorphic Phantoms Used in the MIRD Schema^{16,17}

Organ	Mass (g) of organ in each phantom					
	Newborn (3.4 kg)*	Age 1 (9.8 kg)	Age 5 (19 kg)	Age 10 (32 kg)	Age 15–adult female (55–58 kg)	Adult male (70 kg)
Adrenals	5.83	3.52	5.27	7.22	10.5	16.3
Brain	352	884	1,260	1,360	1,410	1,420
Breasts, including skin	0.205	1.10	2.17	3.65	407	403
Breasts, excluding skin	0.107	0.732	1.51	2.60	361	351
Gallbladder contents	2.12	4.81	19.7	38.5	49.0	55.7
Gallbladder wall	0.408	0.910	3.73	7.28	9.27	10.5
GI tract						
LLI contents	6.98	18.3	36.6	61.7	109	143
LLI wall	7.98	20.6	41.4	70.0	127	167
SI contents and wall	52.9	138	275	465	838	1,100
Stomach contents	10.6	36.2	75.1	133	195	260
Stomach wall	6.41	21.8	49.1	85.1	118	158
ULI contents	11.2	28.7	57.9	97.5	176	232
ULI wall	10.5	27.8	55.2	93.4	168	220
Heart contents	36.5	72.7	134	219	347	454
Heart wall	25.4	50.6	92.8	151	241	316
Kidneys	22.9	62.9	116	173	248	299
Liver	121	292	584	887	1,400	1,910
Lungs	50.6	143	290	453	651	1,000
Ovaries	0.328	0.714	1.73	3.13	10.5	8.71
Pancreas	2.80	10.3	23.6	30.0	64.9	94.3
Remaining tissue	2,360	6,400	13,300	23,100	40,000	51,800
Skin	118	271	538	888	2,150	3,010
Spleen	9.11	25.5	48.3	77.4	123	183
Testes	0.843	1.21	1.63	1.89	15.5	39.1
Thymus	11.3	22.9	29.6	31.4	28.4	20.9
Thyroid	1.29	1.78	3.45	7.93	12.4	20.7
Urinary bladder contents	12.4	32.9	64.7	103	160	211
Urinary bladder wall	2.88	7.70	14.5	23.2	35.9	47.6
Uterus	3.85	1.45	2.70	4.16	79.0	79.0
Whole body	3,600	9,720	19,800	33,200	56,800	73,700

*Total phantom weight.

$$S(r_k \leftarrow r_h) \approx S(r_k \leftarrow r_h) \times \frac{\text{Reference-man total-body mass}}{\text{Patient total-body mass}} \quad (20b)$$

if $r_h = r_k$ and the patient target region (r_k) mass is not available

Equation (20b) is based on the implicit assumption that organ mass is directly proportional to total body mass.

For a tumor-bearing organ, in the case of ¹⁸⁸Re-labeled lipiodol therapy, the liver, adaptation of the MIRD schema is somewhat more complicated. First, the self-irradiation absorbed dose and S factor for the tumor-bearing organ can be separated into their penetrating and nonpenetrating radiation components:

$$D(r_h \leftarrow r_h) \equiv D_p(r_h \leftarrow r_h) + D_{np}(r_h \leftarrow r_h) \quad (21)$$

$$S(r_h \leftarrow r_h) \equiv S_p(r_h \leftarrow r_h) + S_{np}(r_h \leftarrow r_h) \quad (22a)$$

Table 2 ¹⁸⁸Re "Reference-Man" (ie, the 70-kg Adult Male) S Factors (in rad/ μ Ci-hr) for Selected Source Region-Target Region Pairs

Target Region, r_k	Source Region, r_h			
	Liver	Lung	Red Marrow	Other Tissue (Muscle)
Liver	9.5×10^{-4}	9.1×10^{-7}	3.6×10^{-7}	4.1×10^{-7}
Lung	9.4×10^{-7}	1.7×10^{-3}	4.5×10^{-7}	5.0×10^{-7}
Red marrow	5.0×10^{-7}	6.0×10^{-7}	7.5×10^{-4}	6.4×10^{-7}

Adapted from Snyder et al.²¹

$$= S_p(r_h \leftarrow r_h) + \frac{\sum_i (\Delta_{np})_i (\phi_{np})_i (r_h \leftarrow r_h)}{M_h} \quad (22b)$$

$$= S_p(r_h \leftarrow r_h) + \frac{\sum_i (\Delta_{np})_i}{M_h} \quad (22c)$$

$$= S_p(r_h \leftarrow r_h) + \frac{\Delta_{np}}{M_h} \quad (22d)$$

where

$$S(r_h \leftarrow r_h) = \text{the total self-irradiation } S \text{ factor in source and target region } r_h, \\ = 9.4 \times 10^{-4} \text{ rad}/\mu\text{Ci-hr for } ^{188}\text{Re in the reference-man normal liver} \quad (23)$$

$S_p(r_h \leftarrow r_h)$ = the self-irradiation S factor for penetrating radiations in source and target region r_h ,

$S_{np}(r_h \leftarrow r_h)$ = the self-irradiation S factor for nonpenetrating radiations in source and target region r_h ,

$(\Delta_{np})_i$ = the equilibrium dose constant for nonpenetrating radiation i ,

$(\phi_{np})_i(r_h \leftarrow r_h)$ = the self-irradiation absorbed fraction in nonpenetrating radiations for source and target region r_h ,

$$= 1,$$

$$M_h = \text{the mass of the source and target region } r_h, \\ = 1,800 \text{ g for the reference-man normal liver,} \quad (24)$$

and Δ_{np} = the total equilibrium dose constant for nonpenetrating radiations

$$\equiv \sum_i (\Delta_{np})_i \\ = 1.66 \text{ g-rad/Ci-hr for } ^{188}\text{Re.} \quad (25)$$

Therefore,

$$S_p(r_h \leftarrow r_h) = S(r_h \leftarrow r_h) - \frac{\Delta_{np}}{M_h} \quad \text{and} \quad (26a)$$

$$S_p(\text{Normal liver} \leftarrow \text{Normal liver}) \\ = 1.78 \times 10^{-5} \text{ rad}/\mu\text{Ci-hr} \quad (26b)$$

for ¹⁸⁸Re in the reference-man normal liver.

Using Eq. (18a) for ¹⁸⁸Re in the liver, that is, in the normal liver and, the patient-specific self-irradiation S factor for penetrating radiations can then be calculated as follows:

$$S_p(r_h \leftarrow r_h) = \frac{\text{Patient}}{\text{Reference-man}} S_p(r_h \leftarrow r_h) \\ \times \frac{\text{Reference-man target-region } (r_k) \text{ mass}}{\text{Patient target-region } (r_k) \text{ mass}} \quad (27a)$$

$$\text{Patient } S_p(\text{Liver} \leftarrow \text{Liver}) = 1.78 \times 10^{-5} \text{ rad}/\mu\text{Ci-hr} \\ \times \frac{1800 \text{ g}}{\text{Patient liver mass}} \quad (27b)$$

$$= \frac{0.032}{\text{Patient liver mass}}. \quad (27c)$$

For ¹⁸⁸Re in the liver, that is, in the normal liver and tumor, the patient-specific self-irradiation absorbed dose for penetrating radiations is therefore:

$$D_p(\text{Normal Liver} \leftarrow \text{Normal Liver}) \\ \approx S_p(\text{Liver} \leftarrow \text{Liver}) \times \bar{A}_{\text{Liver}} \quad (28a)$$

$$= \text{Patient } S_p(\text{Liver} \leftarrow \text{Liver}) \times \bar{A}_{\text{Liver}} \quad (28b)$$

$$= \text{Patient } S_p(\text{Liver} \leftarrow \text{Liver}) \times \left\{ \bar{A}_{\text{Normal Liver}} + \bar{A}_{\text{Tumor}} \right\}. \quad (28c)$$

The self-irradiation absorbed dose for nonpenetrating radiations in source and target region r_h is:

$$D_{np}(r_h \leftarrow r_h) = \frac{\Delta_{np}}{M_h} \times \bar{A}_h \quad (29)$$

For ¹⁸⁸Re in the liver, therefore, the mean patient-specific self-irradiation absorbed dose to the normal liver for nonpenetrating radiations is:

$$D_{np}(\text{Normal liver} \leftarrow \text{Normal liver}) \\ = \frac{\Delta_{np}}{\text{Patient normal liver mass}} \times \bar{A}_{\text{Normal liver}}. \quad (30)$$

The total absorbed dose to the patient normal liver is simply the sum of $D_p(\text{Normal liver} \leftarrow \text{Normal liver})$, given in Eqs. (27c) and (28c), and $D_{np}(\text{Normal liver} \leftarrow \text{Normal liver})$, given in Eq. (30).

Note that the absorbed dose to the normal liver from penetrating radiations (x - and γ -rays) includes contributions from activity in both the normal liver and from tumor in the liver because of the relatively long distances penetrated by such radiations. In contrast, the absorbed dose from nonpenetrating radiations (β -rays) is contributed only by activity in the normal liver itself because such radiations are completely absorbed within the tumor, that is, cannot penetrate into the surrounding normal liver.

The absorbed dose contribution from activity in the rest of the body, that is, *not* specifically in the liver, lung, and red marrow, also should be included. Muscle, of course, is a tissue distributed throughout the body, and the respective S factors with muscle as the source region can be used to estimate the absorbed dose contributions from the rest of the body to liver, lung, and red marrow:

$$S(r_k \leftarrow \text{Rest of body}) \approx S(r_k \leftarrow \text{Muscle}) \quad (31)$$

The cumulated activity in the rest of the body can be calculated by subtracting the combined cumulated activities in the liver, lung, and red marrow from that in the total body.

The total absorbed doses, $D(\text{Normal liver})$, $D(\text{Lung})$, and $D(\text{Red marrow})$, to the respective at-risk normal tissues, liver, lung, and red marrow, are then calculated by summing the source region absorbed dose contributions:

$$\begin{aligned} D(\text{Normal liver}) &= D(\text{Normal liver} \leftarrow \text{Normal liver with tumor}) \\ &+ D(\text{Liver} \leftarrow \text{Lung}) \\ &+ D(\text{Liver} \leftarrow \text{Red marrow}) \\ &+ D(\text{Liver} \leftarrow \text{Rest of body}) \end{aligned} \quad (32a)$$

$$\begin{aligned} D(\text{Lung}) &= D(\text{Lung} \leftarrow \text{Normal liver with tumors}) \\ &+ D(\text{Lung} \leftarrow \text{Lung}) \\ &+ D(\text{Lung} \leftarrow \text{Red marrow}) \\ &+ D(\text{Lung} \leftarrow \text{Rest of body}) \end{aligned} \quad (32b)$$

$$\begin{aligned} D(\text{Red marrow}) &= D(\text{Red marrow} \leftarrow \text{Normal liver with tumors}) \\ &+ D(\text{Red marrow} \leftarrow \text{Lung}) \\ &+ D(\text{Red marrow} \leftarrow \text{Red marrow}) \\ &+ D(\text{Red marrow} \leftarrow \text{Rest of body}) \end{aligned} \quad (32c)$$

The total absorbed doses to the at-risk normal tissues are then normalized to the scout administered activity (mCi) to yield the respective absorbed doses per unit administered activity (rad/mCi). Based on the absorbed doses per unit administered activity (rad/mCi) thus calculated, the actual therapeutic activity to be administered is the *minimum* value among those activities projected to deliver the maximum tolerated absorbed doses to the respective at-risk normal tissues—3,000 rad to liver, 1,200 rad to lung, and 150 rad to red marrow.

Tumor Dosimetry

Tumor dosimetry is not a component of the maximum-tolerated-activity approach to radionuclide therapy or of the MIRD schema. Nonetheless, tumor absorbed doses can be estimated using data already required for normal-tissue dosimetry. One approach to dosimetry is the classical “geometric-factor” method^{2,23}:

$$D(\text{Tumor} \leftarrow \text{Tumor}) = D_p(\text{Tumor} \leftarrow \text{Tumor}) + D_{np}(\text{Tumor} \leftarrow \text{Tumor}) \quad (33a)$$

$$\begin{aligned} &= \frac{0.0346 \times \Gamma \times \bar{g} \times T_p \times (A_o)_{\text{Tumor}}}{\text{Tumor mass}} \\ &+ \frac{\Delta_{np}}{\text{Tumor mass}} \times \bar{A}_{\text{Tumor}} \end{aligned} \quad (33b)$$

where $D(\text{Tumor} \leftarrow \text{Tumor}) =$ the self-dose, that is, the tumor-to-tumor absorbed dose,

$D_p(\text{Tumor} \leftarrow \text{Tumor}) =$ the self-dose, that is, the tumor-to-tumor absorbed dose, for penetrating raduations,

$D_{np}(\text{Tumor} \leftarrow \text{Tumor}) =$ the self-dose, that is, the tumor-to-tumor absorbed dose, for nonpenetrating raduations,

$\Gamma =$ the specific gamma ray constant (rad-cm²/μCi-h),

and $\bar{g} =$ the mean geometric factor

$$= 3\pi r \quad (34)$$

where $r =$ the radius (cm) of the tumor (assumed to be spherical).

As noted previously, the entire algorithm has been automated using an Excel spreadsheet, which performs the necessary calculations and incorporates all the pertinent reference data.

Conclusion

Radiation dosimetry deals with the determination of the amount and the spatial and temporal distribution of energy deposited in matter by ionizing radiation. Internal radionuclide radiation dosimetry specifically deals with the deposition of radiation energy in tissue due to a radionuclide within the body. However, unlike external radiation dose (which can often be measured), internal radiation dose must be calculated. These procedures have evolved for more than 60 years from relatively simple approaches to those with a high level of sophistication. This report has presented the basic concepts and practical computational approaches to patient-specific internal radiation dosimetry for intrahepatic artery ¹⁸⁸Re-labeled lipiodol for treatment of liver cancer. Although conceptually straightforward, the computations presented are tedious. Importantly, beginning with CT- or MRI-derived organ and masses, and organ and total-body activities (from gamma camera imaging) as input data, all pertinent calculations can be performed with an Excel spreadsheet. Further, all necessary reference data (eg, reference-man organ masses, equilibrium dose constants, S factors) are readily available and can be incorporated into such a spreadsheet to fully automate the dose-calculation process.

Intrahepatic artery lipiodol localizes in liver tumors and, when labeled with ¹³¹I, is efficacious in their treatment. It is expensive and not widely available, especially in the developing parts of the world in which liver cancer is endemic. Lipiodol labeled with generator-produced, β-emitting ¹⁸⁸Re (17 hours; $E_\beta = 0.53\text{--}0.70$ MeV; range = 4 mm), is a convenient, cost-effective alternative. The ¹⁸⁸Re-lipiodol dosimetry protocol described has been implemented worldwide in the International Atomic Energy Agency’s Coordinated Research Project on radionuclide treatment of liver cancer. As described in detail elsewhere in this issue, the trial in which this dosimetry methodology was employed comprised 185 patients from 8 countries, including China, Colombia, India, Mongolia, the Philippines, Singapore, Thailand, and Vietnam. Patient age ranged from 22 to 84 years (median 55 years, mean 55.4 years, SD 11.8 years). There were 146

(79%) men and 39 (21%) women. Of the 185 patients, to date 145 have sufficient information available for dosimetric analysis. A single treatment was given to 134 patients (72%), 42 patients (23%) received 2 treatments, 8 (4%) received 3 treatments, and 1 patient received 4 treatments. The total administered activity (including the scout dose) during the first treatment ranged from 21 to 363 mCi (mean: 108 mCi, median 100 mCi; SD 54 mCi). In 32% of the patients, the dose-limiting organ was the lungs whereas in the other 68%, it was the liver. In all the patients that received less than the maximum dose to lungs or liver, there was no dose-limiting toxicity. Only one patient received more than the maximum pulmonary radiation absorbed dose; there was transient pulmonary toxicity in this patient. Two other patients developed pulmonary toxicity after the second treatment dose; the cumulative pulmonary radiation absorbed dose in these patients was less than the maximum permissible dose. However, the effect of cumulative radiation to the lungs cannot be estimated from the available data. Moreover, several factors, including baseline performance status and extent of disease and pulmonary function before each treatment, as well as interval between treatments, will effect pulmonary toxicity. With basic instrumentation (planar gamma camera, well counter) available in most developing countries, a patient-specific maximum-tolerated activity treatment planning algorithm for ¹⁸⁸Re-lipiodol therapy of liver cancer can be implemented and largely automated.

References

1. Sgouros G: Treatment planning for internal emitter therapy: Methods, applications and clinical implications, in Schlafke-Stelson A, Stabin M, Sparks R (eds): Proceedings of the Sixth International Radiopharmaceutical Dosimetry Symposium (ORISE 99-0164). Oak Ridge, TN, U.S. Dept of Energy and Oak Ridge Associated Universities, 1999, pp 13-25
2. Zanzonico P, Brill A, Becker DV: Radiation dosimetry, in Wagner W, Szabo Z, and Buchanan J (eds): Principles of Nuclear Medicine (ed 2). Philadelphia, PA, W.B. Saunders Co, 1995, pp 106-134
3. Zanzonico P, Edwards C, Sgouros G, et al: Practical dosimetry: Quantitative imaging in radionuclide therapy, in Adelstein S, Kassis AI, Burt RW (eds): Dosimetry of Administered Radionuclides. Washington, DC, American College of Nuclear Physicians/Department of Energy, 1989, pp 275-294
4. Furhang EE, Larson SM, Buranapong P, et al: Thyroid cancer dosimetry using clearance fitting. *J Nucl Med* 40:131-136, 1999
5. Benua R, Cicale N, Sonenberg M: The relation of radioiodine dosimetry to results and complications in the treatment of metastatic thyroid cancer. *Am J Roentgenol* 87:171-182, 1962
6. Kaminski MS, Zasadny KR, Francis IR, et al: Radioimmunotherapy of B-cell lymphoma with [131I]anti-B1 (anti-CD20) antibody. *N Engl J Med* 329:459-465, 1993
7. Kaminski MS, Zasadny KR, Francis IR, et al: Iodine-131-anti-B1 radioimmunotherapy for B-cell lymphoma. *J Clin Oncol* 14:1974-1981, 1996
8. Wahl RL, Zasadny KR, MacFarlane D, et al: Iodine-131 anti-B1 antibody for B-cell lymphoma: An update on the Michigan Phase I experience. *J Nucl Med* 39:215-275, 1998
9. Zasadny K, Gates VL, Fisher SJ, et al: Correlation of dosimetric parameters with hematological toxicity after radioimmunotherapy of non-Hodgkin's lymphoma with I-131 anti-B1. Utility of a new parameter: "Total body dose-lean". *J Nucl Med* 36:214P, 1995
10. Weber D, Eckerman KF, Dillman LT, et al: MIRD: Radionuclide Data and Decay Schemes, New York, Society of Nuclear Medicine, 1989, p 447
11. Madsen MT, Park CH, Thakur ML: Dosimetry of iodine-131 ethiodol in the treatment of hepatoma. *J Nucl Med* 29:1038-44, 1988
12. Nakajo M, Kobayashi H, Shimabukuro K, et al: Biodistribution and in vivo kinetics of iodine-131 lipiodol infused via the hepatic artery of patients with hepatic cancer. *J Nucl Med* 29:1066-1077, 1988
13. Sgouros G, Jureidini IM, Scott AM, et al: Bone marrow dosimetry: Regional variability of marrow-localizing antibody. *J Nucl Med* 37:695-8, 1996
14. Siegel J, Wessels BW, Watson EE, et al: Bone marrow dosimetry and toxicity in radioimmunotherapy. *Antibody Immunocon Radiopharm* 3:213-223, 1990
15. Sgouros G: Bone marrow dosimetry for radioimmunotherapy: Theoretical considerations. *J Nucl Med* 34:689-694, 1993
16. Snyder W, Ford MR, Warner GG, et al: Estimates of absorbed fractions for monoenergetic photon sources uniformly distributed in various organs of a heterogeneous phantom. Medical Internal Radiation Dose (MIRD) Pamphlet No 5. *J Nucl Med* 10:5-52, 1969 (suppl 3)
17. Cristy M, Eckerman K: Specific absorbed fractions of energy at various ages from internal photon sources (I-VII). Oak Ridge National Laboratory Report ORNL/TM-8381/V1-7, Springfield, VA, National Technical Information Service, Dept of Commerce, 1987
18. Zanzonico PB, Bigler RE, Sgouros G, et al: Quantitative SPECT in radiation dosimetry. *Semin Nucl Med* 19:47-61, 1989
19. Jaszczak R, Greer RJ, Floyd CE, et al: Improved SPECT quantitation using compensation for scattered photons. *J Nucl Med* 25:893-900, 1984
20. Loevinger R, Budinger TF, Watson EE, et al: MIRD Primer for Absorbed Dose Calculations. New York, Society of Nuclear Medicine, 1991
21. Snyder W, Ford MR, Warner GG, et al: "S," Absorbed Dose Per Unit Cumulated Activity for Selected Radionuclides and Organs. Medical Internal Radiation Dose (MIRD) Pamphlet No 11. New York, Society of Nuclear Medicine, 1975
22. Zanzonico PB: Internal radionuclide radiation dosimetry: A review of basic concepts and recent developments. *J Nucl Med* 41:297-308, 2000
23. Marinelli L, Quimby E, Hine G: Dosage determination with radioactive isotopes. I. Fundamental dosage formulae. *Nucleonics* 2:56-66, 1948